

Fig. 1.

until we approach wide bandwidth, the dark current noise is greater. The thermal noise power is  $kTB$ . The dark current output noise power is  $2q_i a B_D R$ . Hence, for the dark current noise to be greater, we must have

$$2q_i a B_D R > kTB_D. \quad (2)$$

The value of  $R$  is limited by the required time constant of the circuit. If we have to pass  $B_D$ , and have a circuit capacity of  $C$ , then for baseband systems,

$$R \approx \frac{1}{B_D C} \text{ ohms.} \quad (3)$$

As the bandwidth requirements increase,  $R$  decreases and the thermal noise power can no longer be ignored. The NEP does not take into account this thermal noise because it is specified for 1-c/s bandwidth, and for 1 c/s, the dark current noise in photodiodes will always be greater than the thermal noise. In general, for all optical and IR detectors the NEP or  $D^*$  will not be a function of the thermal noise because of the narrow reference bandwidth.

By means similar to the concept employed in determining the NEP, we can determine the equivalent input power for which the signal current  $i_s = i_{nt}$ , the thermal noise current. At  $i_s = i_{nt}$ , we have

$$i_s^2 = \frac{4kTB_D}{R}, \quad (4)$$

and hence for  $\epsilon =$  quantum efficiency and  $f =$  the optical frequency,

$$P = \left( \frac{hf}{eq} \right) \frac{2\sqrt{kTB_D}}{\sqrt{R}} \text{ watts} \quad (5)$$

where the maximum resistance  $R$  will be limited by the required time constant of the circuit. Thus,

$$P = \frac{hf}{eq} 2\sqrt{kT} B_D \sqrt{C} \text{ watts.} \quad (6)$$

If, as in the case of the NEP, we define the signal current equal to the thermal noise current for 1-c/s bandwidth, we can denote this incident power as the Thermal Equivalent Power (TEP) such that the

$$\begin{aligned} \text{TEP} &= \frac{hf}{eq} 2\sqrt{kTC} \\ &= \frac{3.2 \times 10^{-26} f \sqrt{TC}}{\epsilon} \frac{\text{watts}}{\text{c/s}}. \end{aligned} \quad (7)$$

Note that the minimum discernible signal (MDS) will be a function of the TEP, NEP, and the bandwidth. The MDS will be given by

$$\text{MDS} = \sqrt{B_D} \sqrt{(\text{NEP})^2 + (\text{TEP})^2 B_D} \text{ watts.} \quad (8)$$

Equation (8) reveals that as bandwidth increases the thermal noise term can be more significant than the detector shot noise. When

$$B_D = \left( \frac{\text{NEP}}{\text{TEP}} \right)^2 \text{ c/s} \quad (9)$$

the two noise sources are of equal magnitude. The physical reason for the greater influence of the thermal noise with increased bandwidth is that the output resistance must be lower, and hence the output signal power and shot noise power is decreased.

The factors determining the TEP are frequency, temperature, quantum efficiency, and capacity. For wide bandwidth conditions, and for high quantum efficiency, it can be shown that the thermal noise becomes significant even for low temperatures. For example, consider  $T = 4^\circ\text{K}$ ,  $\epsilon = 1$ ,  $f = 3 \times 10^{14}$ , and  $B_D = 100$  mc/s. With an assumed capacity of 2 pF,  $R_{\text{max}} \approx 5000$  ohms. Thus,  $(\text{TEP})^2 B_D$  will become greater than  $(\text{NEP})^2$  for NEP less than approximately  $10^{-11}$  watts/c/s<sup>1/2</sup>.

The point should be made that from the foregoing it is seen that the TEP of a detector as a function of wavelength, as well as the NEP, should be given in order that the detector sensitivity can be realistically determined for a given bandwidth. Values of TEP for selected conditions are shown in Fig. 1.

The foregoing expression for TEP is not valid for the case of detectors that possess post-detection gain unless the gain factor is taken into account. To include these cases, a general expression for the TEP can be given as

$$\text{TEP} = \frac{hf}{eq} \frac{2\sqrt{kTC}}{G_c} \frac{\text{watts}}{\text{c/s}} \quad (10)$$

where  $G_c$  is the equivalent current gain of the detector.

MONTE ROSS<sup>1</sup>  
McDonnell Aircraft  
St. Louis, Mo.

<sup>1</sup> Mr. Ross was formerly with the R&D Dept. of Hallicrafters Co., Chicago, Ill.

## An Integratable Time-Variable Gyrator

Since the most promising methods of time-variable network synthesis [1], as well as some aspects of analysis [2], rely heavily on the time-variable transformer [3] and, since transformers can be constructed by cascading gyrators, a practical realization of a time-variable gyrator has some interest. It also appears that any integrated circuit realization of a gyrator would be of considerable interest because inductors can be obtained through capacitor loading [4]. Here we present a gyrator realization which allows time-variable gyration resistances and which appears natural for integrated circuitry.

The circuit is that of Fig. 1 which is analyzed as follows. Considering only signal components, the direct connection of the load  $Z_L$  to transistor  $T_1$  allows  $V_2$  to appear directly across  $R_a$ . Since, to a good approximation,  $I_1$  flows through  $R_a$ ,

$$V_2 = R_a I_1. \quad (1)$$

Thus,  $T_1$  acts as a current to voltage converter. In comparison,  $T_2$  acts as a voltage

inverter, when  $R_2=R_1$  is chosen to place  $-V_1$  on the base, and hence the emitter, of  $T_3$ . If now we choose

$$R_0 \gg |Z_i| \quad (2)$$

then  $I_2$  is, to a good approximation, the current through  $R_0$ . The transistor  $T_3$  is then also a current to voltage converter and, observing polarities,

$$V_1 = -R_0 I_2. \quad (3)$$

When

$$R_a = R_b \quad (4)$$

(1) and (3) describe a gyrator. In conclusion, for loads satisfying (2) the circuit between the source and the load of Fig.1 behaves as a gyrator.

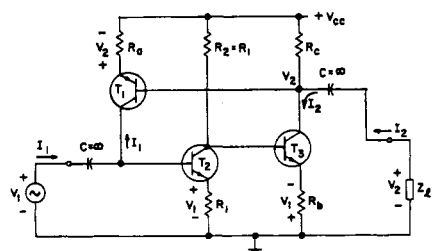


Fig. 1. Gyrator circuit.

To make the device time-variable one can simply vary  $R_a=R_b$ . Many ways of accomplishing this are available, but probably the most satisfying is to use the source-to-drain resistance of a field effect transistor [5] operated below pinch-off. As shown in Fig. 2, this yields a linear resistance, over a reasonable range, which can be easily varied by varying the gate voltage.

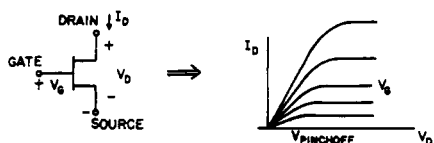


Fig. 2. Field-effect characteristics to obtain variable resistance,  $V_D < V_{pinchoff}$ .

Of course, various practical considerations must be taken into account for physical construction. However, the circuit has been constructed in nonintegrated form and has worked rather satisfactorily. It should be observed that a disadvantage of the circuit is that  $R_b=R_a$  needs to be chosen. However, in many situations one does not actually require a gyrator and (1) and (3) are sufficient (without  $R_b=R_a$ ). Likewise, the realization of a time-variable transformer as the cascade of two gyrators only requires that one of the gyrators be time-variable.

#### ACKNOWLEDGMENT

The authors are indebted to Prof. D. O. Pederson for his encouragement on the project.

W. NEW  
R. NEWCOMB  
Stanford Electronics Labs.  
Stanford, Calif.

#### REFERENCES

- [1] D. A. Spaulding, "Lossless time-varying impedance synthesis," *Electronics Letters*, vol. 1, pp. 165-167, August 1965.
- [2] B. D. Anderson, D. A. Spaulding, and R. W. Newcomb, "Useful time-variable circuit-element equivalences," *Electronics Letters*, vol. 1, pp. 56-57, May 1965.
- [3] —, "The time-variable transformer," *Proc. IEEE (Correspondence)*, vol. 53, p. 634, June 1965.
- [4] R. W. Newcomb, "Topological analysis with ideal transformers," *IEEE Trans. on Circuit Theory*, vol. CT-10, pp. 457-458, September 1953.
- [5] D. O. Pederson, *Electronic Circuits* (preliminary ed.), New York: McGraw-Hill, pp. 18-23.

#### Polynomial Approximation of the Fermi Integral

In recent years there has been an increasing desire by workers in the semiconductor device field to treat the more complex problems of degenerate semiconductors. These problems occur in heavily doped semiconductors or at low temperatures. The analysis of these problems has been neglected partially because they involve the Fermi integral—a tabulated function. With the availability of high speed digital computers, it is now possible to analyze many of these problems by numerical methods. The fact that the Fermi integral is a tabulated function is of much less consequence. A relatively simple means of calculating the integral with minimum time and computer storage is desirable.

This correspondence presents a group of polynomials by which the Fermi integral and its derivatives may be calculated quickly and with a high degree of accuracy. Polynomial approximations do exist for certain ranges of the function [1]. For arguments less than zero, and for large positive arguments, analytical expressions may be used [2]. However, in the region just below zero an excessive number of terms is required, and just above zero the analytical expression has poor accuracy (100 percent error in some cases). The region near zero is of the greatest importance in degenerate semiconductors. Some empirical expressions do exist for these regions but these have errors which are quite intolerable if difference methods are employed in the computation.

The polynomial approximations described herein to represent the Fermi integral for arguments between  $-1.0$  and  $12.0$  have an rms relative error of  $0.000093$  percent and a maximum relative error of  $0.000243$  percent. The rms error in the sixth significant figure is  $0.334$  with a maximum error of  $1.356$ . These errors are calculated using the table of McDougall and Stoner [1] as reference.

The polynomials are easily differentiated. The differentiated polynomials have an rms relative error of  $0.00093$  percent, a maximum relative error of  $0.0023$  percent, an rms sixth significant figure error of  $3.24$ , and a maximum sixth significant figure error of  $10.4$ .

The polynomials covering arguments less than  $-1.0$  and greater than  $12.0$  are those

described in the literature [1] and have smaller errors than those specified above.

Strictly speaking, the Fermi integral is given by

$$F_{1/2}(x) = \int_0^{\infty} \frac{y^{1/2}}{1 + e^{-x-y}} dy.$$

In semiconductor application it is more convenient to evaluate

$$F(x) = \frac{1}{\Gamma(1/2)} \int_0^{\infty} \frac{y^{1/2}}{1 + e^{-x-y}} dy.$$

These differ only by the quantity  $\Gamma(1/2) = \sqrt{\pi}$ . This integral converges to  $\exp(x)$  for  $x \ll 0$ . With this definition, using a parabolic approximation for the energy surfaces, the densities of free holes and electrons are given by

$$\begin{aligned} n &= P_1 F(E_F/E_T) \\ p &= P_2 F(-(E_0 + E_F)/E_T) \end{aligned} \quad (1)$$

where

$$P_1 = 4.831 \times 10^{15} \left[ \left( \frac{m_e}{m_0} \right) T (^{\circ}\text{K}) \right]^{3/2} \text{cm}^{-3}$$

$$P_2 = 4.83 \times 10^{15} [(m_h/m_0) T (^{\circ}\text{K})]^{3/2} \text{cm}^{-3}$$

$m_0$  = rest mass of an electron

$m_e$  = electron mass

$m_h$  = hole mass

$E_F$  = Fermi level with the conduction band at  $E = 0$ .

$E_0$  = energy gap.

$E_T = T (^{\circ}\text{K})/11\,605.9 \text{ eV}$ .

When the semiconductor is nondegenerate ( $E_F/E_T$  sufficiently negative), (1) reduces to simply  $n = P_1 \exp(E_F/E_T)$ . The Fermi integral can be represented by an exponential within the specified accuracy for arguments less than  $-12.5$ . The typical Fermi level  $4E_T$  below the conduction band taken in analytical calculations has an error of  $0.65$  percent or  $1/174$  in the sixth significant figure. Usually this is tolerable if differences are not taken.

The accuracy of the differentiated polynomial is an indication of the smoothness of the polynomial approximation. Aside from this satisfying fact the first derivative of the Fermi integral is quite useful. An application in degenerate semiconductors is the relationship between the diffusion constant and the mobility—the Einstein relation. This subject has been of recent concern in communications to the PROCEEDINGS OF THE IEEE [3], [4]. Using (1) to express the electron or hole density the Einstein relation may be shown to be [5]

$$D = E_T \mu \frac{F(x)}{F'(x)}$$

where  $\mu$  is the carrier mobility,  $D$  is the diffusion constant, and  $F'(x)$  is the first derivative of the Fermi integral. The quantity  $x$  is  $E_F/E_T$  for electrons and  $-(E_0 + E_F)/E_T$  for holes.

The coefficients of the two analytical polynomials and the four polynomials computed by the OSU IBM 7094 digital computer are listed below. The polynomial curve fitting subprogram was furnished by the Numerical Computation Laboratory of